LANGMUIR

pubs.acs.org/Langmuir Article

Organized Hybrid Molecular Films from Natural Phospholipids and Synthetic Block Copolymers: A Physicochemical Investigation

Arianna Balestri, Leonardo Chiappisi,* Costanza Montis, Samantha Micciulla, Barbara Lonetti,* and Debora Berti

Cite This: *Langmuir* 2020, 36, 10941−10951 Read Online

ACCESS | Metrics & More | Article Recommendations | Supporting Information

ABSTRACT: In the last few years, hybrid lipid-copolymer assemblies have attracted increasing attention as possible two-dimensional (2D) membrane platforms, combining the biorelevance of the lipid building blocks with the stability and chemical tunability of copolymers. The relevance of these systems varies from fundamental studies on biological membrane-related phenomena to the construction of 2D complex devices for material science and biosensor technology. Both the fundamental understanding and the application of hybrid lipid-copolymer-supported bilayers require thorough physicochemical comprehension and structural control. Herein, we report a comprehensive physicochemical and structural characterization of hybrid monolayers at the air/water interface and of solid-supported hybrid membranes constituted by 1,2-dipalmitoyl-*sn*-glycero-3-phosphocholine (DPPC) and the block copolymer poly(butadiene-*b*-ethyleneoxide) (PBD-*b*-PEO). Hybrid lipid-copolymer supported bilayers (HSLBs) with variable copolymer contents were prepared through spontaneous rupture and fusion of hybrid vesicles onto a hydrophilic substrate. The properties of the thin films and the parent vesicles were probed through dynamic light scattering (DLS), differential scanning calorimetry (DSC), optical ellipsometry, quartz crystal microbalance with dissipation monitoring (QCM-D), and confocal scanning laser microscopy (CSLM). Stable, hybrid lipid/copolymer systems were obtained for a copolymer content of 10−65 mol %. In particular, DSC and CSLM show lateral phase separation in these hybrid systems. These results improve our fundamental understanding of HSLBs, which is necessary for future applications of hybrid systems as biomimetic membranes or as drug delivery systems, with additional properties with respect to phospholipid liposomes.

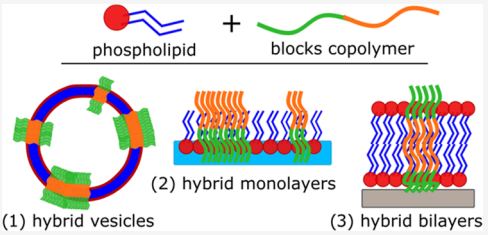

INTRODUCTION

Phospholipids are the primary structural components of biological membranes, and their self-assembly into fluid bilayers acts as a barrier and exchange site between the internal and external cellular compartments. In aqueous solution, both natural and synthetic phospholipids can spontaneously assemble into bilayered closed structures, leading to the formation of liposomes.[1] Due to their high biocompatibility and their structural similarity with plasma membranes, liposomes have been widely used both as drug delivery systems for applications in nanomedicine and as biomimetic membranes for fundamental studies on cell-membrane-related phenomena in simplified conditions.[2,3]

Among the multiple applications of lipid assemblies, their two-dimensional (2D) projection on a support to form supported lipid bilayers (SLBs) has been widely exploited, mainly to build mimics of biological membranes, for biophysical studies on cell-membrane-related phenomena.[4] Recently, thanks to the progress in surface patterning methods, microfluidics, or organic electronics, supported lipid films have also been highlighted for their potential as substrate-mediated soft devices.[5] Bilayer deposition onto solid surfaces has the advantage to preserve the native lipid state while providing a robust and stable platform to characterize the system with sensitive surface techniques, including quartz crystal microbalance with dissipation monitoring (QCM-D), optical ellipsometry, atomic force microscopy (AFM), and neutron or X-ray reflectivity (NR or XRR).[6−8]

If, on the one hand, lipid assemblies can adapt to external stimuli and environmental changes, i.e., pH or ionic strength, they are, on the other hand, often characterized by mechanical fragility and the lack of stability. In addition, the synthetic versatility and possibility to conjugate functional moieties to phospholipids are limited, thereby narrowing their applicative range.

A totally synthetic alternative to phospholipids is represented by amphiphilic block copolymers, which can self-assemble in robust vesicular structures called polymersomes.[9,10] Due to the higher chemical versatility of copolymers with respect to phospholipids and to the higher stability with respect to liposomes, polymersomes gained a growing interest

Received: May 27, 2020
Revised: August 26, 2020
Published: August 27, 2020

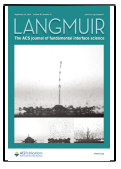

https://dx.doi.org/10.1021/acs.langmuir.0c01544
Langmuir 2020, 36, 10941−10951

in membrane research, both as biomimetic systems and as vectors for drug delivery.[11−13] Polymer bilayers offer significant chemical, spatial and physicochemical variability, e.g., their membrane thicknesses typically vary from 8 to 50 nm, compared to the 4−5 nm thickness typical of phospholipid bilayers.[14] In addition, the wide choice of block chemistry and the possibility of varying both blocks lengths allow structures with the desired tunable properties to be designed.[6] While polymer bilayers exhibit a higher mechanical stability with respect to lipid ones, their membranes are characterized by a low permeability, low lateral mobility, and minor biocompatibility, which limits their use in biological studies.[15]

In this context, hybrid bilayers, obtained as a mixture of lipids and copolymers, have the potential not only to merge the advantages of lipo- and polymer membranes[16−20] but also to present new biophysical and biochemical properties.[21]

In particular, the addition of a copolymer can (i) improve the stability and mechanical strength of the mixed membrane, compared to the bare lipid one; (ii) allow a wide range tunability of the thickness of the membrane, which could more easily host hydrophobic species (as hydrophobic nanoparticles or membrane proteins); (iii) strongly influence membrane transport properties and curvature and in some case induce channels in the lipid membrane; and (iv) promote the formation of complex membranes, with lateral phase separation and coexistence of domains of different fluidities (see Figure 1). The strategy of introducing heterogeneities into membranes to impart complex, multifunctional properties is widely exploited by nature, where lateral membrane inhomogeneities mediate various cellular processes in cells. From a material science standpoint, new sophisticated devices with domains organized in a controlled way, responsive or differently functionalized, with a spatial and temporal control of the properties, are fascinating.

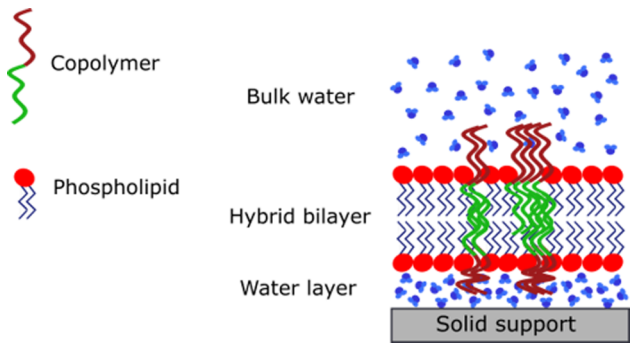

Figure 1. Schematic diagram of a solid-supported hybrid lipid-copolymer bilayer.

While the formation and the physicochemical, structural characterization of SLBs have been addressed in many studies over the years, the inclusion of amphiphilic copolymers into SLBs to form hybrid lipid-copolymer supported bilayers (HSLBs) has been developed only very recently.[21−23] For the aim of designing biologically relevant model membranes, hybrid lipid-copolymer systems have been studied as a platform for direct membrane protein insertion in free-standing membranes or monolayers.[6,24,25]

In this work, we performed a complete physicochemical characterization of HLSBs made of poly(butadiene-*block*-ethyleneoxide) (PBD-*b*-PEO) and 1,2-dipalmitoyl-*sn*-glycero-3-phosphocholine (DPPC). DPPC, a common component of biological membranes in lungs, is an interesting component for the design of thermoresponsive nanocarriers, thanks to its melting transition temperature close to physiological temperature (T_m = 41 °C).[26] Recently, PBD-*b*-PEO systems have been proposed for biomedical applications,[5] as they can self-assemble into structures similar to lipids thanks to the presence of hydrophilic (PEO) and hydrophobic (PBD) groups. The polymer has the ratio of hydrophilic to total mass that falls in the range (29−39%) suitable for creating vesicles and a low glass transition temperature (T_g = −10 °C), which ensures dispersion and mixing with lipids.[21] Although PBD is not biodegradable, the conjugation with PEO makes the block copolymer PBD-*b*-PEO biocompatible.[27] Based on the hydrophobic effect and the self-assembly of the amphiphilic copolymer, it has been shown that the synthetic polymer PBD-*b*-PEO can be incorporated into lipid bilayers.[21−23] In a bilayer structure, DPPC and PBD-*b*-PEO form 4.4 nm lipid[28] and 10−12 nm polymer[21] membranes, respectively.

Previously, the formation of fluidlike inhomogeneities in mixed PBD-*b*-PEO and DPPC membranes was evidenced at the microlength scale.[29] In this contribution, the lateral phase separation in lipid-rich and copolymer-rich regions is addressed, combining a series of surface techniques in monolayers, supported bilayers, and free-standing bilayers.

The lipid−copolymer interactions were analyzed at the air/water interface through isothermal cycles and at the solid/water interface thorough quartz crystal microbalance with dissipation monitoring (QCM-D) and confocal laser scanning microscopy (CSLM), while their structural properties were investigated using optical ellipsometry at both interfaces.

EXPERIMENTAL SECTION

Materials. 1,2-dipalmitoyl-*sn*-glycero-3-phosphocholine (DPPC) (>99%) and *β*-bodipy(2-(4,4-diuoro-5,7-dimethyl-4-bora-3*a*,4*a*-diaza-sindacene-3-pentanoyl)-1hexadecanoyl-*sn*-glycero-3-phosphocholine) used for liposomes and supported hybrid bilayers were purchased from Avanti Polar Lipids, Inc. (Alabaster, AL). The copolymer polybutadiene (M_n = 2500 g/mol)-*block*-poly(ethylene oxide) (M_n = 1300 g/mol) (1,2 addition butadiene, 89%) (PBD-*b*-PEO) and the rhodamine-labeled copolymer polybutadiene (M_n = 1200 g/mol)-*block*-poly(ethyne oxide) (M_n = 600 g/mol), RhodPEBD-*b*-PEO, were purchased from Polymer Source. NaCl and $CaCl_2 \cdot H_2O$ salts used for solution preparation were purchased from Sigma and Merck, respectively.

Preparation of Vesicles. Vesicles were prepared with the method of dry film rehydration.[30] Briefly, solutions of the pure lipids, copolymer, and lipid/copolymer blends were prepared in a chloroform mixing stock solution of 5 mg/mL DPPC and 5 mg/mL PBD-*b*-PEO in $CHCl_3$. The solvent was removed using nitrogen flux to obtain films. Complete solvent removal was achieved by keeping the film under vacuum for 24 h. Hybrid vesicles were prepared in both aqueous and 0.1 M NaCl solutions to determine the effective formation of hybrid DPPC/PBD-*b*-PEO vesicles as preliminary characterization and as the buffer condition for HSLB deposition, respectively. Then, 4 mL of Milli-Q water and 0.1 M NaCl aqueous solution was added and the film was rehydrated through sonication at 50 °C for 15 min, obtaining a final concentration of 1 mg/mL for all of the samples. Aqueous suspensions were extruded nine times at 50 °C through 100 nm pore size polycarbonate membrane filters using an Avanti Mini-Extruder. The dispersions in 0.1 M NaCl solution, consisting of large agglomerates, were then tip-sonicated with a Digital Sonifier Model 450 (Branson, Hampton, NH), provided with a horn tip (diameter 25.4 mm), in an intermittent-pulse mode (5 s), with a power of 40 kHz (amplitude 100%). Vesicles were formed with the following molar ratios of the copolymer and lipid: 0, 10, 35, 65, and 100 mol % PBD-*b*-PEO/DPPC.

https://dx.doi.org/10.1021/acs.langmuir.0c01544
Langmuir 2020, 36, 10941−10951

Hybrid Monolayers at the a/w Interface. Monolayers at the air/water interface were prepared by depositing chloroform solutions (15−50 μL) with copolymer/lipid molar ratios of 0, 10, 35, 65, and 100 mol % PBD-*b*-PEO/DPPC (1 mg/mL) onto a pure Milli-Q water surface (subphase). Experiments were performed after 20 min to allow the chloroform to evaporate.

Preparation of Supported Bilayers. Solid-supported bilayers were prepared by vesicles' spontaneous rupture and fusion onto a 2 cm × 2 cm Si/SiO_2 wafer. Before vesicle deposition, the surface of the wafer was made hydrophilic with a sonication bath for 20 min in an ethanol solution, nitrogen drying, and UV-ozone cleaning for 15 min. SLBs were obtained by adding a 10 mM aqueous $CaCl_2$ solution to the dilute (0.5−1 mg/mL) dispersions of vesicles in a 0.1 M NaCl solution and subsequently deposited onto a silicon substrate at T = 50 °C for 30 min. After deposition, the substrate was washed 15 times with 1 mL of Milli-Q water and then cooled to ambient temperature.

METHODS

Dynamic Light Scattering (DLS). Dynamic light scattering (DLS), used to evaluate the *Z*-average size and polydispersity of the aqueous suspension vesicles or liposomes, was performed using a Brookhaven Instruments apparatus (BI 900AT correlator and BI 200 SM goniometer). The light source was the second harmonic of a diode Nd:YAG laser, λ = 532 nm, Coherent DPY315M-100, linearly polarized in the vertical direction. The normalized intensity time autocorrelation of the scattered light was measured at 90° and analyzed according to the Siegert relationship, which connects the first-order or field-normalized autocorrelation function $g_1(q, \tau)$ to the measured normalized autocorrelation function $g_2(q, \tau)$

$$g_2(q, \tau) = 1 + \beta |g_1(q, \tau)|^2 \quad (1)$$

with β spatial coherence factor, which depends on the geometry of the detection system. The field autocorrelation functions (ACFs) were analyzed through a cumulant analysis stopped at the second order and through reverse Laplace transform performed with the Contin algorithm.[31] Measurements were performed at 25 °C three times for each sample diluted to 0.5 mg/mL to avoid multiple scattering. The reported size is the average from the three measurements with standard deviation.

Differential Scanning Calorimetry (DSC). Measurements were performed with a micro-DSC III 106 (Setaram, France). Cells made of Hallestoy C (volume of 1 cm^3) were filled with ∼400 mg of a hybrid vesicle solution (2−8 mg/mL) and the reference cell with the same amount of 0.1 M NaCl and 10 mM $CaCl_2$ solution. In addition, the copolymer vesicles and liposomes were also measured (2 mg/mL). During the operation, a constant nitrogen flux purged the instrument and scans were performed between 10 and 60 °C with three heating and two cooling cycles with a heating rate of 0.5 °C/min. The data were corrected for the empty cell contribution using pyDSC,[32] freely available at https://github.com/leonardo-chiappisi/pyDSC, which computes the baseline according to Malakhov et al.[33]

Compression Isotherms. The compression isotherms of pure and hybrid monolayers at the air−water interface were measured on a Langmuir trough, 300 mm × 200 mm, with a Teflon compression barrier (NIMA 611). The surface pressure, $\Pi = \Upsilon_{a/w} - \Upsilon_{a/m}$, was monitored with a Wilhelmy plate made of filter paper during two compression/expansion cycles, performed with a constant barrier speed of 25 mm/min. After 20 min from the deposition, for the evaporation of chloroform, two isothermal cycles were applied at constant temperature T = 21 °C.

Monolayer Surface Excess. The surface excess of pure and hybrid monolayers as a function of surface pressure was determined using a Langmuir trough KSV-Nima, 19.5 cm × 5 cm, with two symmetrical compression barriers with a constant compression of 1 mm/min, in combination with a phase-modulated picometer light ellipsometer (Beaglehole Instruments, New Zealand) equipped with a HeNe laser with λ = 632.8 nm, at an angle of incidence in the range of 51−55°.

The physical information of the sample was extracted using an optical model based on classical electromagnetic theory and the approximation of the sample in terms of parallel optical slabs of defined thicknesses (d) and refractive indexes (n). The air−water interface was characterized using three parallel layer model (bulk water, monolayer, and air). Due to the low thickness of the monolayer, optical ellipsometry cannot be used to resolve simultaneously both the film thickness d and its refractive index. However, it is possible to extract the surface excess Γ at determined pressure values with a Wilhelmy plate using the formula[34]

$$\Gamma = \frac{d(n_1 - n_2)}{\frac{\partial n}{\partial c}} \quad (2)$$

where n_1 and n_2 are the refractive indexes of the monolayer and the aqueous subphase, respectively; d is the thickness of the monolayer; and $\partial n/\partial c$ is the refractive index increment. The refractive index increment of the components in water, $\partial n/\partial c$, was experimentally measured for the pure samples (DPPC and PBD−PEO) using a differential refractometer DR3 by SLS Systemtechnik. The refractive index increment of the hybrid samples was calculated as the mass-weighted average of the pure components. The surface excess was then obtained by fitting the value of the thickness. The refracting index of the monolayer was calculated by extrapolation of $\partial n/\partial c$ to $c \rightarrow \rho$ with ρ being the density of the monolayer, arbitrary fixed to 1 g/cm^3. This value was arbitrarily chosen, but the choice, however, had no sensible effect on the resulting surface excess values obtained. The values of the thickness d were evaluated by fitting the experimental angles Ψ and Δ using the pyEllip python script, freely available at https://github.com/leonardo-chiappisi/pyEllip. The script uses lmfit[35] and tmm[36] python packages.

Quartz Crystal Microbalance with Dissipation. Quartz crystal microbalance with dissipation monitoring (QCM-D) was performed with a Q-Sense E4 instrument (Q-Sense, Gothenburg, Sweden), equipped with four flow liquid cells (0.5 mL internal volume), each containing a coated quartz sensor, with a 5 MHz fundamental resonance frequency, mounted horizontally. The active surface of the sensors (≈1 cm^2) was coated with a thin SiO_2 layer (≈100 nm thick). The sensors were cleaned before use by washing in pure ethanol and bath sonication for 15 min, nitrogen drying, and finally ozone cleaning for 10 min. The experiments were performed at 40 °C, and solvent exchange in the measurement chamber was achieved with a peristaltic pump. The sensors were placed in the chambers, and Milli-Q water was injected at a low flow rate (0.1 mL/min). The fundamental resonance frequencies (f) and corresponding energy dissipation factors (D) were measured for the odd overtones (3rd−11th). A stable baseline for both f and D of the different harmonics was ensured before the injection of the vesicles at a low flow rate (0.1 mL/min). The QCM-D curves reported are normalized by the overtone number. The hydrated mass was estimated by applying the Sauerbrey relation,[37] valid under the approximation of rigid films

$$\Delta m = -\frac{C\Delta f}{n} \quad (3)$$

with mass sensitivity constant C = 17.7 ng/(cm^2 Hz) for a 5 MHz sensor crystal. Each experiment was performed in duplicate.

Optical Ellipsometry of SLB. The ellipsometry data of SLB were recorded using a Beaglehole ellipsometer described earlier. For each sample, three measurements at different positions on the sample were performed at a variable angle in a range between 50 and 80°. The values of the thickness d and the refractive index n were evaluated by fitting the experimental angles Ψ and Δ as described earlier.

The solid-supported bilayer was characterized using a four-layer model, consisting of the bulk silicon layer, a SiO_2 layer, the bilayer, and bulk water. The SiO_2 layer thickness was determined prior to sample deposition and was kept constant during the analysis of the supported lipid bilayer data.

Confocal Laser Scanning Microscopy (CLSM). Confocal microscopy was performed on a Leica TCS SP8 confocal microscope (Leica Microsystems). β-Bodipy and RhodPBD-*b*-PEO were excited,

https://dx.doi.org/10.1021/acs.langmuir.0c01544
Langmuir 2020, 36, 10941−10951

respectively, at 488 nm, with an Ar laser, and 561 nm, with a DPSS 561 laser. The fluorescence was collected with PMTs in the wavelength ranges 498−550 and 600−650 nm, for β-bodipy and RhodPBD-*b*-PEO, respectively. The fluorescent probes in the vesicle solution were added to a ratio dye of 0.1% (w/w). All of the measurements were performed at room temperature (T = 25 °C).

RESULTS AND DISCUSSION

Hybrid Vesicles. Due to their amphiphilic nature, DPPC and PBD-*b*-PEO molecules can individually assemble into vesicular aggregates, forming liposomes and polymersomes, respectively.[38,39] To study the mixing behavior of the lipid and the synthetic diblock copolymer in vesicle membranes, different molar mixtures between DPPC and PBD-*b*-PEO were prepared and characterized through DLS and differential scanning calorimetry (DSC).

As a preliminary characterization, with the aim to verify their hybrid nature, vesicles with different copolymer contents (0, 35, 65, and 100 mol % PBD-*b*-PEO) were prepared in aqueous solution by the extrusion method and investigated by DLS (Figure 2). The autocorrelation functions (ACFs) of the scattered intensity were analyzed through the cumulant fitting stopped to the second order, highlighting the formation of monodisperse vesicles for all systems: DPPC (Dh = 114 ± 1 nm, PDI 0.109), hybrid 35 mol % PBD-*b*-PEO/DPPC (Dh = 98 ± 1 nm, PDI 0.212), hybrid 65 mol % PBD-*b*-PEO/DPPC (Dh = 93 ± 1 nm, PDI 0.226), and pure PBD-*b*-PEO (Dh = 76.6 ± 0.5 nm, PDI 0.129). These results suggest that PBD-*b*-PEO spontaneously self-assemble into vesicles of smaller size (76.6 nm hydrodynamic diameter) with respect to the mesh size of the extrusion membrane (100 nm), while DPPC vesicles are, as expected, slightly larger (114 nm). When mixed, the obtained vesicles are characterized by the Z-averaged intermediate size (98−93 nm), as also clearly visible from the trend of the normalized ACFs reported in Figure 2a, suggesting the successful formation of hybrid copolymer-lipid vesicles.

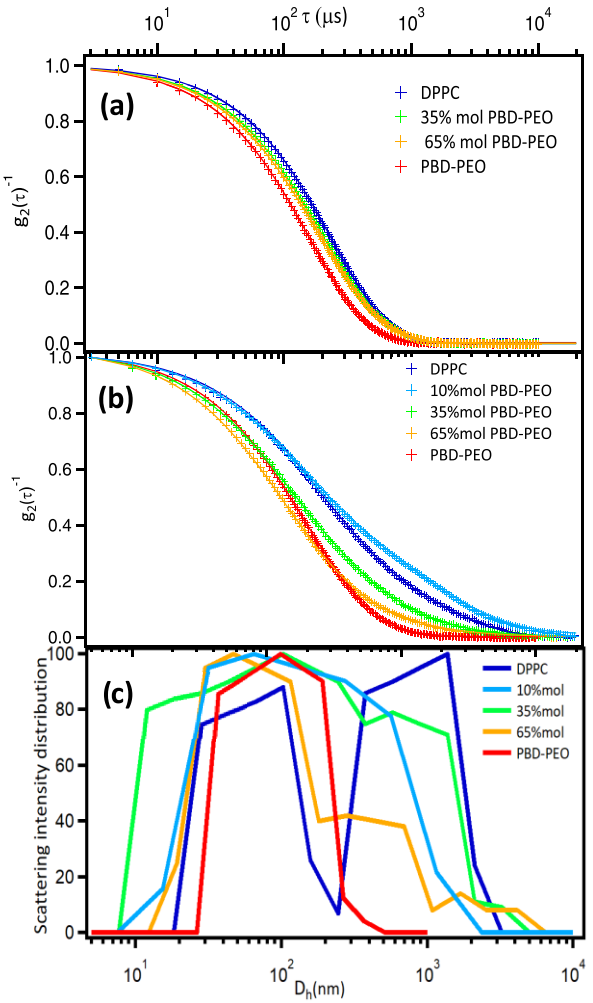

Figure 2. Normalized intensity correlation function of 0, 35, 65, and 100 mol % poly(butadiene-*b*-ethyleneoxide)/1,2-dipalmitoyl-*sn*-glycero-3-phosphocholine (PBD-*b*-PEO/DPPC) in water (a) and of 0, 10, 35, 65, and 100 mol % PBD-*b*-PEO/DPPC in 0.1 M NaCl (b) and their histograms of the intensity distribution recorded in NaCl solution (c).

As the hybrid vesicles have to be used for SLB deposition through vesicle fusion, we decided to characterize them in the buffer of choice for this procedure, 0.1 M NaCl. Pure and hybrid vesicles of different compositions (0, 10, 35, 65, and 100 mol % PBD-*b*-PEO) were prepared in 0.1 M NaCl (see the Experimental Section for details). Vesicles in salt solution consisted of large agglomerates that cannot be extruded but only tip-sonicated, creating polydisperse vesicles. The autocorrelation functions are shown in Figure 2b. The Contin method was applied to analyze the autocorrelation functions of the pure lipid and hybrid dispersions (results shown in Figure 2c), while cumulant analysis stopped to the second order was applied to the pure polymer dispersion, revealing monodisperse polymersomes with a hydrodynamic radius of 104 ± 6 nm and PDI 0.174. This result confirms that the PBD-*b*-PEO copolymer spontaneously tends to self-assemble into relatively monodisperse vesicles, which are only slightly larger than those obtained in Milli-Q water and prepared by extrusion. Conversely, both DPPC and hybrid systems are characterized by a very broad size distribution. In all cases, stable systems up to two weeks with particle sizes between 50 and 2000 nm are found. DPPC, being a zwitterionic phospholipid, tends to form multilamellar vesicles of broad size distribution; Contin analysis highlights the presence of two main distinct populations, the first one being centered at around 100 nm (small vesicles) and the second one centered at around 1000 nm (large multilamellar vesicles and/or aggregates). Interestingly, the hybrid systems show an intermediate behavior between pure PBD-*b*-PEO vesicles and DPPC vesicles, with the second larger population gradually disappearing as the percentage of the copolymer with respect to lipids in the hybrid increases (see Figure 2c). This is further evidence of the effective formation of hybrid lipid/copolymer aggregates.

In summary, DLS data prove that hybrid polydisperse vesicles are formed in 0.1 M NaCl solution in all of the copolymer range investigated (0−100% PBD-*b*-PEO/DPPC) and that the obtained aggregates are likely to be hybrid systems, containing both lipid and copolymer components. These hybrid vesicles, even if polydisperse, are suitable for the formation of HSLB.

To investigate more in detail the mixing thermodynamics of DPPC and PBD-*b*-PEO in the hybrid vesicles, we performed DSC experiments on the same systems.

Differential scanning calorimetry (Figure 3) was performed on dilute aqueous dispersions of pure and hybrid DPPC/PBD-*b*-PEO vesicles to probe their thermotropic behavior. The thermograms show two distinct phase transitions: the DPPC pretransition and the main phase transition.[40,41] The

https://dx.doi.org/10.1021/acs.langmuir.0c01544
Langmuir 2020, 36, 10941−10951

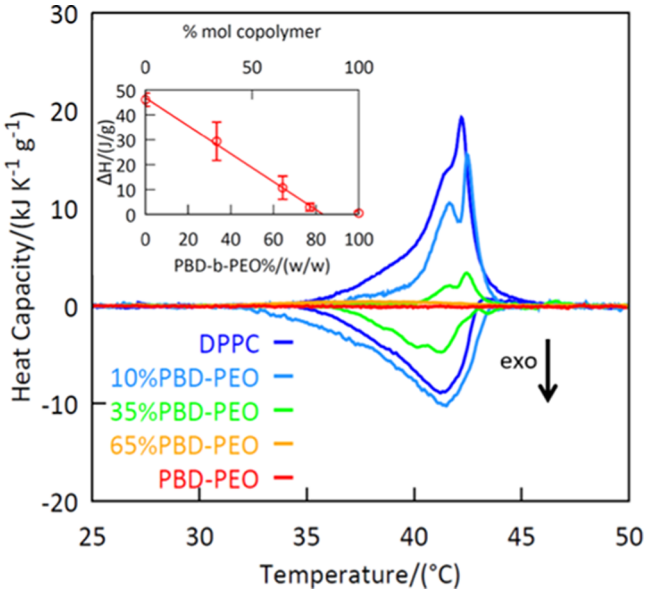

Figure 3. DSC thermograms of 0, 10, 35, 65, and 100 mol % PBD-*b*-PEO/DPPC. The heat capacity normalized by the mass of the sample (polymer plus lipid) is reported as a function of temperature. The third heating profile (heat rate of 0.5 °C/min) and the second cooling profile (cooling rate of 0.5 °C/min) are reported. The inset represents the dependence of the melting enthalpy on the weight content of the copolymer in the vesicle mixture.

pretransition ripple phase, (P_β), is visible for $T < 41$ °C up to a copolymer content of 35 mol %. The data show that the DPPC main transition temperature from the gel to the liquid-crystalline phase occurs at $T \approx 41$ °C[42] and it is not affected by the presence of the block copolymer. No melting transition is observed for the 65 mol % hybrid vesicle and for the pure block copolymer system. Moreover, the melting enthalpy shows a linear decrease as a function of the lipid content (Table 1).

Table 1. Phase-Transition Properties of the Samples, Melting Temperature (T_m) (Determined as the Peak Maximum of the Heating Process), and the Melting Enthalpy ΔH Normalized by the Mass of the Sample (Lipids Plus the Block Copolymer)

sample	mass fraction PBD−PEO (%)	T_m (°C)	ΔH (J/g_{tot})	ΔH (J/g_{DPPC})
DPPC	0	41 ± 1	46 ± 3	46 ± 3
10 mol % PBD-*b*-PEO	33	41 ± 1	29 ± 12	33 ± 2
35 mol % PBD-*b*-PEO	64	40 ± 1	10 ± 5	27± 13
65 mol % PBD-*b*-PEO	77	NA	NA	NA
100 mol % PBD-*b*-PEO	100	NA	NA	NA

The persistence of both gel and ripple phases up to 65 mol % of the copolymer, the negligible decrease of T_m, and the linear relationship between melting enthalpy and lipid content clearly indicate a lateral phase separation, where domains of pure DPPC coexist with domains of the block copolymer not involved in the phase transition. As the block copolymer content increases, the DPPC melting domains possibly decrease in number and/or size. As the inset of Figure 3 shows, from the intercept of ΔH vs the copolymer mass fraction, we identify a threshold amount of PBD−PEO for the observation of the phase transition, corresponding to 80% w/w, which can be interpreted as due to partial miscibility between the copolymer and the phospholipid at the nanoscale. On the other hand, we can interpret the linear dependence of the melting enthalpy on the PBD−PEO content, as consistent with the presence of a layer of lipid molecules, located at the grain boundaries of the different domains in the bilayers whose packing order is disrupted by the proximity with copolymer domains. Therefore, these interfacial lipids will not contribute to melting. With the assumption that the copolymer domains are disklike with a radius R_{cop}, the dependence of the melting enthalpy on the copolymer content can be described with the following equation (see SI for derivation and further assumptions)

$$\Delta H_m = \Delta H_m^0 \left[1 - \chi_{cop}\left(\frac{(R_{cop} + d)^2}{R_{cop}^2}\right)\right] \quad (4)$$

where ΔH_m^0 is the melting enthalpy in the absence of the copolymer, d the thickness of the region of DPPC perturbed by the presence of PBD-*b*-PEO, and χ is the surface fraction of the copolymer approximated by its mass fraction. From a linear fit of the experimental ΔH_m values, we determine a typical size for the copolymer domains of 2827 nm^2, assuming a perturbation thickness of 1.6 nm, corresponding to two molecules of DPPC with a headgroup area of 0.5 nm^2.[28]

In summary, the DLS study on vesicles' dispersions shows that hybrid lipid/copolymer vesicles are present for all of the lipid/copolymer ratios investigated. From DSC data, we infer that in these vesicles the lipid and the copolymer show only partial miscibility, with lateral phase separation into lipid and copolymer-rich nanoregions. To gain deeper insight into the miscibility between DPPC and PBD-*b*-PEO, we investigated mixed monolayers at the air/water interface, as detailed in the following section.

Hybrid Monolayers at the Air−Liquid Interface. According to previous studies,[43,44] the monolayer's properties at the air/water interface can elucidate the bilayer's ones in the vesicles. To achieve a deep knowledge of the hybrid DPPC/PBD-*b*-PEO systems, monolayers at the air/water interface were investigated at the same lipid/copolymer molar ratio (0, 10, 35, 65, and 100 mol % PBD-*b*-PEO) of the hybrid vesicles.

The phase behavior of the hybrid lipid-copolymer monolayers at the air/liquid interface was investigated using the Langmuir trough technique, with pure water as a subphase; see data in Figure 4. Two isothermal cycles, performed at T = 21 °C, show a good stability of the system, with only the pure block copolymer showing the loss of material (full isothermal compression/expansion cycles are given in Figure S3 in the SI). The DPPC monolayer shows the typical feature of the Π−*A* isotherm for this lipid: as the area per molecule was reduced, an increasing packing of the homogeneous liquid-expended (LE) phase occurred; at an area per molecule of about 60 Å^2, the typical plateau corresponding to the coexistence of LE/liquid-condensed (LC) phases and a highly ordered liquid-condensed (LC) phase was observed; finally, at a small value of the area per molecule (50 Å^2), only the LC phase was present. Considering the DPPC headgroup area of 50 Å^2, the corresponding bilayer's pressure can be calculated trough the DPPC monolayer Π−*A* curve, giving a value of 27 mN/m.

For PBD−PEO, the surface pressure isotherm spans over a larger range of molecular areas due to its bigger size. The

https://dx.doi.org/10.1021/acs.langmuir.0c01544
Langmuir 2020, 36, 10941−10951

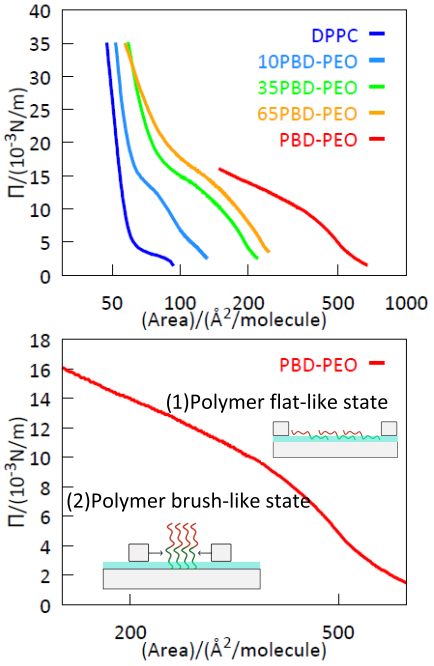

Figure 4. Π−*A* isotherms of 0, 10, 35, 65, and 100 mol % (top) PBD-*b*-PEO/DPPC monolayers in the Milli-Q water subphase and the extended 100 mol % PBD-*b*-PEO/DPPC isotherm (bottom). The data refer to the first compression performed at T = 21 °C, and the complete data of the two compression/expansion cycles are reported in the SI. Note the logarithmic *x*-axis.

copolymer adopts two preferential conformations, with the transitional conformation behavior typical for block copolymers:[45] at a very large area per molecule (Π < 10 mM/m), the block copolymer takes a flatlike state while a brushlike state appears at a high pressure (Π > 10 mM/m). Indeed, the transition appears at the critical pressure of the hydrophilic block, Π_0 = 10 mM/m, for PEO. At surface pressure higher than Π_0, the PEO block is squeezed out from the interface and the brush state is formed: this regime is dominated by entangling interactions at moderate pressure and a terminal repulsive regime at high packing.[46] The copolymer monolayer could not be compressed to a surface pressure beyond 20 mN/m, while previous studies reported a maximum surface pressure of 30 mN/m.[47,48] We assume that this difference is a purely instrumental limit due to the ratio between the deposited material and the minimum available area for the compression of the monolayer. As shown in Figure 4, the hybrid monolayers show an intermediate behavior with respect to the two pure systems. In particular, all of them present the flatlike to brushlike state transition typical of the copolymer and the steep increase of the surface pressure at low area per molecule typical of DPPC and the isotherms shift toward larger areas with respect to DPPC with increasing amounts of the copolymer in the mixture. The effective formation of hybrid monolayers was further confirmed, comparing the area per molecules close to the collapse with the calculated ones from the literature values for the pure phospholipid and copolymer monolayers (50 and 100 Å^2, respectively). The area values determined from the isotherms are in good agreement with the calculated ones with a single exception for the 65 mol % PBD−PEO monolayer as can be observed in Table 2.

Table 2. Experimental and Calculated Areas per Molecules for Hybrid Monolayers

hybrid monolayer	calculated area (Å^2/molecule)	experimental area (Å^2/molecule)
10 mol % PBD-*b*-PEO	54	52
35 mol % PBD-*b*-PEO	63	60
65 mol % PBD-*b*-PEO	70	57

From the experimentally measured Π−A profiles, the surface compressive modulus, E_s, of the monolayer was determined via the following expression[49]

$$E_s = \frac{1}{C_s} = -A\left(\frac{d\Pi}{dA}\right)_T \quad (5)$$

where C_s is the monolayer compressibility, A is the area per unit molecule at a given lateral stress, and Π is the corresponding lateral pressure. The dependence of E_s on the surface pressure (Figure 5) shows that the film elasticity is

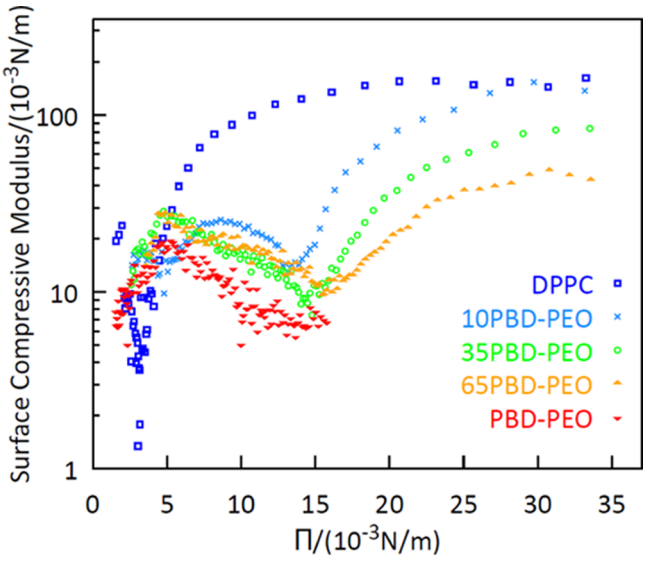

Figure 5. Surface compressive modulus of 0, 10, 35, 65, and 100 mol % PBD-*b*-PEO/DPPC isotherms of the first compression (the surface compressive moduli of the isotherms of the complete cycles are in the SI).

dominated by the phospholipid at high lateral pressure, with values of E_s close to 0.1 N/m, suggesting that the confinement of the polymer chains induces the monolayers' stiffness in a similar way as the lipopolysaccharides at the air−water interface.[49,50] Interestingly, the presence of the block copolymer causes a softening of the hybrid monolayers, depending on its content probably because it increases the mean distance between DPPC molecules. At low lateral pressure, the elasticity of the film is dominated by the properties of the block copolymer: a clear minimum, characteristic of phase-transitions[51] is found at Π ∼ 15 mN/m and is ascribed to a conformational change of the copolymer.

The surface excess, Γ, at the air−liquid interface was monitored as a function of lateral pressure by multiangle ellipsometry combined with a Langmuir through, displayed in

https://dx.doi.org/10.1021/acs.langmuir.0c01544
Langmuir 2020, 36, 10941−10951

Figure 6. The ellipsometric data are given in the Supporting Information in Figure S6.

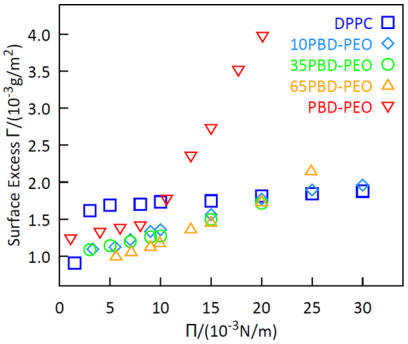

Figure 6. Surface excess Γ dependence on the lateral pressure Π for 0, 10, 35, 65, and 100 mol % PBD-*b*-PEO/DPPC monolayers.

Figure 6 displays the surface excess Γ of the monolayers at the air/water interface at different lateral pressures Π (0−30 mN/m). The pure DPPC monolayer has a sudden increase of Γ, from 0.8 to 1.6 mg/m^2, in the range of 0−5 mN/m; then, it presents a slight increase until 30 mN/m. The surface excess of the pure PBD−PEO monolayer, on the contrary, increases slightly in the range 0−10 mN/m (1.3−1.7 mg/m^2) and then it has a sudden increase, reaching a value of 4 mg/m^2. Hybrid monolayers have a surface excess Γ that reflects the pure copolymer monolayer surface excess until the critical value Π = 10 mN/m, where the trend becomes the same as the phospholipid. The surface excess Γ presents a nonlinear profile at a constant lateral pressure: hybrid monolayers have a surface excess lower than those of the pure lipid and copolymer monolayers when the surface pressure is Π = 10 mN/m, while with the increase of the surface pressure (Π = 20 mN/m), their surface excess assumes a constant value like the DPPC, indicating that the monolayers became more rigid because of the repulsive interactions between the lipid tails. We can conclude that at low-pressure values (Π < 10 mN/m) the interactions between the copolymer chains dominate at the interface, while with the increasing pressure (Π > 10 mN/m) the repulsion between the phospholipid tails determines the interfacial behavior.

The ensemble of data on free-standing bilayers and monolayers proves that the DPPC/PBD−PEO system forms hybrid monolayer and lamellar systems, with the partial miscibility of the phospholipid in a copolymer-rich phase. For copolymer contents from 10 to 65 mol %, distinct regions of lipid and copolymer phases are formed within the bilayers.

Therefore, DPPC−PBD−PEO systems appear as interesting hybrid materials combining characteristics of both building blocks (e.g., thermoresponsivity, lateral compressibility, etc.). To further extend this investigation, we addressed the formation of hybrid supported bilayers on a hydrophilic solid substrate.

Hybrid Supported Copolymer-Lipid Bilayers. Solid-supported bilayers were prepared by vesicle fusion on a hydrophilic SiO_2 substrate at a constant temperature T = 40 °C, close to the gel-to-liquid-crystalline phase-transition temperature (T_m = 41 °C) of the phospholipid. QCM-D was used to follow the vesicle adsorption and fusion;[52] measurements were performed at T = 40 °C in 0.1 M NaCl and 10 mM $CaCl_2$. QCM-D data shown in Figure 7 highlight that vesicle

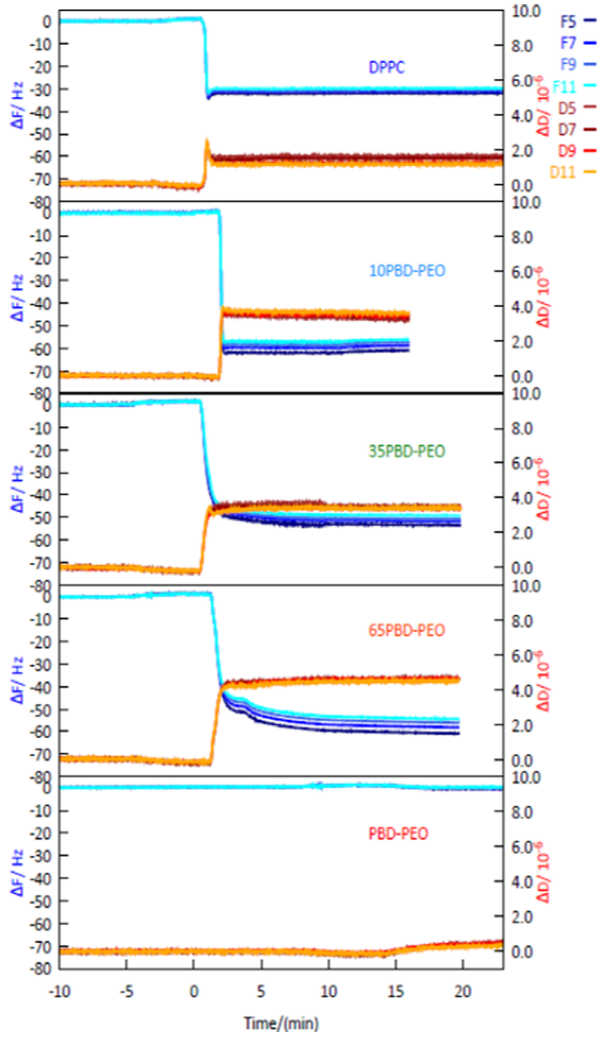

Figure 7. QCM-D measurements of the adsorption and desorption of 0, 10, 35, 65, and 100 mol % PBD-*b*-PEO/DPPC in 0.1 M NaCl and 10 mM $CaCl_2$.

adsorption and fusion take place only in the presence of DPPC. In contrast, no film is formed when the crystal is exposed to a solution of a pure block copolymer, consistent with the literature.[53] In particular, pure DPPC systems are characterized by frequency shifts and dissipation typical of a supported lipid bilayer, that is, around −30 Hz frequency shift and low dissipation, consistent with a homogeneous SLB firmly coupled to the support.[54]

Conversely, hybrid systems are characterized by higher frequency shifts and dissipation, indicating a more hydrated membrane with a lower coupling with the sensor surface. This evidence clearly proves that a hybrid membrane is formed on the support, with structural/viscoelastic properties that differ from both the pure DPPC and the pure copolymer. In particular, the lower coupling of the membrane with the support can be assigned to the thickness mismatch between the copolymer and the lipid moieties, which might induce the formation of localized lifted areas partially detached from the surface. This characteristic is particularly attractive for specific applications of the hybrid SLB, for instance, the insertion/reconstitution of functional membrane proteins, which is a generally challenging task in lipid SLBs, due to the attachment of the lipid membrane to the underlying support.

https://dx.doi.org/10.1021/acs.langmuir.0c01544
Langmuir 2020, 36, 10941−10951

To quantitatively estimate the hydrated mass of the bilayer, we applied the Sauerbrey relation,[37] which describes purely elastic responses and can be safely applied when $\Delta D/\Delta f \ll 0.4 \times 10^{-6}$ Hz^{-1} [55] (for the plot, see Figure 8). Consistent with the qualitative observations above discussed, the adsorbed mass for the pure copolymer is negligible; for DPPC, it is estimated as 0.5 μg/cm^2, which is consistent with a homogeneous coverage of the support by the lipid membrane;[8] the hybrid films exhibit the largest adsorbed mass (1 μg/cm^2), attributable to the efficient thin film formation and to the large coupling with water of the copolymer inserted in the bilayer structure. In particular, the maximum adsorbed mass observable in Figure 8 is a result of efficient film formation in the presence of DPPC in the mixture and of the strong coupling of the copolymer hydrophilic block with water.

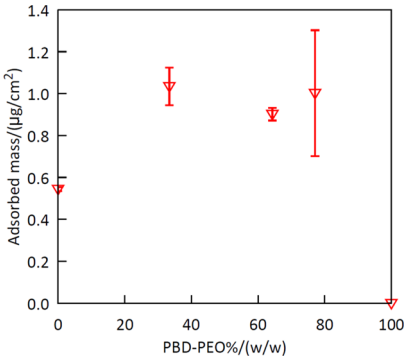

Figure 8. Adsorbed mass estimate with the QCM-D technique at different PBD−PEO concentrations (w/w).

The thickness of solid-supported bilayers was determined via a multiangle ellipsometric experiment, using classical electromagnetic theory in conjunction with the parallel layer model consisting of a silicon/silicon oxide/bilayer/water structure. The treatment assumes that the total sample consists of parallel slabs; each one is a uniform material of homogeneous composition described by a single set of optical constants (refractive index n and thickness d). To reduce the number of parameters, the thickness of the SiO_2 layer was determined on a clean substrate and kept constant for the analysis of the SLB samples. The obtained values of film thickness and refractive index are reported in Table 3.

A pure polymer layer on the silicon substrate was not prepared, not having observed absorption with the QCM-D. The pure DPPC and the hybrid SLBs exhibit very similar thicknesses of approximately 6.6 nm and a refractive index of 1.49. The results confirm the formation of a solid supported bilayer for all of the investigated samples.[22] The minimal change in thickness as a function of the copolymer content indicates that the adsorbed dry mass remains constant within the investigated sample series. This result is in good agreement with the QCM-D results (Figure 8), which show a moderate increase in mass with the presence of the copolymer, which we ascribe to the water coupled to the hydrophilic moieties of the macromolecule.

Table 3. Estimated Thicknesses for the Parallel-Slabs Optical Model

layer	thickness (nm)	refractive index
air	∞	1.00
water	∞	1.33
DPPC	6.3 ± 0.3	1.495 ± 0.002
10 mol % PBD-*b*-PEO/DPPC	6.8 ± 0.3	1.488 ± 0.003
35 mol % PBD-*b*-PEO/DPPC	6.5 ± 0.3	1.480 ± 0.003
65 mol % PBD-*b*-PEO/DPPC	6.6 ± 0.3	1.477 ± 0.003
SiO_2	2.9 ± 0.3	1.46
Si	∞	3.98

Confocal laser scanning microscopy (CLSM) was employed to evaluate the formation and the morphology of mixed bilayers generated by vesicle rupture and fusion on a transparent support of borosilicate. To investigate the morphology of the film at the microscale, and in particular the possible presence of lipid-rich and of copolymer-rich regions, we used two different fluorescent probes: a rhodamine-modified copolymer (RhodPBD-*b*-PEO) and a lipid β-bodiby dye. The dyes differ in their relative affinity toward the lipid and copolymer phases, and they have an amphiphilic nature, so they spontaneously embed in the vesicle bilayer. Moreover, they are characterized by well-separated absorption and emission spectra: rhodamine is excited at a wavelength of 561 nm, and its emission spectra lie in the range of 571−630 nm; in contrast, the β-bodipy excitation wavelength is 488 nm and it emits in the range 488−530 nm. The different spectral properties allow the simultaneous monitoring of the distribution of the two species. CLSM experiments were also performed on pure samples of DPPC and PBD-*b*-PEO doped with the two fluorescent dyes as control measurements reported in SI. All of the CLSM images highlight a uniform fluorescent probe lateral distribution, suggesting the successful supported bilayer formation on a slide by the vesicle rupture and fusion at the microscale. The CLSM images of hybrid samples show clear red and green patterns, evidencing a phase separation in lipid- and copolymer-rich regions at the microscale. From a qualitative point of view, a clear correlation appears between the relative amount of the copolymer and the lipid in the mixed membrane in the resulting phase separation extent at the micron scale in lipid- and copolymer-rich regions, as can be visualized from the CLSM images (Figure 9).

In conclusion, all of the CLSM images highlight the formation of a micron-scale defect-free (lack of uncovered areas and/or vesicles) thin film with a microscopic phase separation into copolymer-rich and lipid-rich regions, suggesting the successful supported bilayer formation on the slide by vesicle rupture and fusion at the microscale. From the study of simple systems constituted of hybrid vesicles and monolayers to the more complicated hybrid supported bilayers, a phase separation is highlighted at the nano- and the microscale, where hybrid materials combine the inherent properties of the DPPC and PBD−PEO components.

SUMMARY AND CONCLUSIONS

In this work, a comprehensive physicochemical characterization of hybrid lipid-copolymer systems, made of DPPC phospholipid and PBD-*b*-PEO amphiphilic block copolymer, is presented. The properties of the aqueous vesicle solutions, of the monolayer at the air/water interface, and of the solid-supported bilayers were investigated. DSC proved the successful formation of the hybrid vesicles, clearly showing nonmixing behavior at the nanoscale. All of the data (optical ellipsometry, QCM-D) confirm HSLB formation upon vesicle rupture and fusion on a silicon substrate with an effective incorporation of the copolymer in the lipid layer. The 2D characterization of the mixed membrane at the micron scale

https://dx.doi.org/10.1021/acs.langmuir.0c01544
Langmuir 2020, 36, 10941−10951

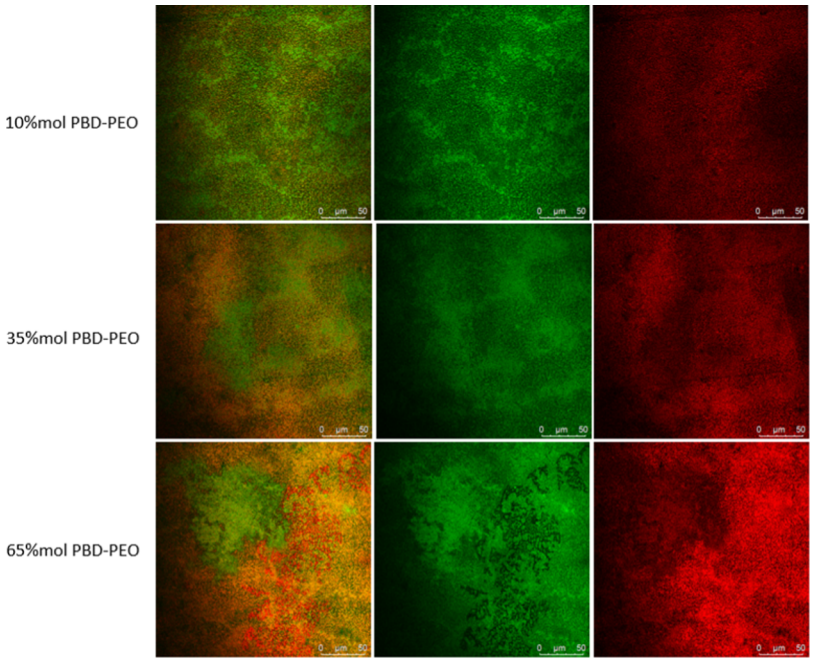

Figure 9. CLSM images for hybrid 10, 35, and 65 mol % PBD-*b*-PEO/DPPC SLBs. Merged and single channels PBD(1200)-*b*-PEO(600) + rhodamine excitation wavelength 561 nm, emission wavelength 571−630 nm (red), *β*-bodipy excitation wavelength 488 nm, and emission wavelength 488−530 nm (green).

was estimated using CLSM. It confirms the successful formation of HSLBs also on a borosilicate cover glass as a support, showing the presence of a lateral phase separation in distinct lipid- and copolymer-rich regions at the micron scale, which is qualitatively dependent on the relative amounts of the two components. Microphase separation has been evidenced in both the hybrid vesicles and supported lipid bilayer as also observed in the case of GUVs. Polymer inclusion in lipid systems enhances the physicochemical properties of the lipid systems: compression isotherms indicate the realization of softer films with the copolymer in the monolayer. The property dependence of the mixtures on the relative amounts of the two components opens the possibility of fine-tuning the properties of the hybrid, by simply varying the relative lipid-copolymer composition. Overall, these results represent the first physicochemical and structural characterization of DPPC/PBD-*b*-PEO HLSBs, which will be necessary for the future exploitation of HLSBs both in fundamental studies and in applications, i.e., protein or nanoparticle incorporation in the membrane of the bilayers.

■ ASSOCIATED CONTENT

Supporting Information

The Supporting Information is available free of charge at https://pubs.acs.org/doi/10.1021/acs.langmuir.0c01544.

Histograms of the intensity distribution for vesicles in water; derivation of eq 4; complete Π−*A* isothermal cycles; surface compressive modulus for the complete isothermal cycles; refractive index increments for pure DPPC and PBD-*b*-PEO solutions; ellipsometric studies for all of the monolayers; QCM-D-sensed mass for the supported bilayers; ellipsometric studies for all of the supported bilayers; and CSLM images for pure DPPC and PBD-*b*-PEO bilayers (PDF)

■ AUTHOR INFORMATION

Corresponding Authors

Leonardo Chiappisi − *Institut Laue Langevin, 38000 Grenoble, France;* orcid.org/0000-0002-4594-2865; Email: chiappisil@ill.eu

Barbara Lonetti − *Laboratoire des IMRCP, Université de Toulouse, CNRS UMR 5623, Université Toulouse III- Paul Sabatier, F-31062 Toulouse, France;* orcid.org/0000-0003-4291-6861; Email: lonetti@chimie.ups-tlse.fr

Authors

Arianna Balestri − *Department of Chemistry "Ugo Schiff" and CSGI, 50019 Florence, Italy; Institut Laue Langevin, 38000 Grenoble, France*

Costanza Montis − *Department of Chemistry "Ugo Schiff" and CSGI, 50019 Florence, Italy;* orcid.org/0000-0001-6960-3772

Samantha Micciulla − *Institut Laue Langevin, 38000 Grenoble, France*

Debora Berti − *Department of Chemistry "Ugo Schiff" and CSGI, 50019 Florence, Italy;* orcid.org/0000-0001-8967-560X

Complete contact information is available at: https://pubs.acs.org/10.1021/acs.langmuir.0c01544

Author Contributions

The manuscript was written through contributions of all authors. All authors have given approval to the final version of the manuscript.

Notes

The authors declare no competing financial interest.

■ ACKNOWLEDGMENTS

The Partnership of Soft Condensed Matter (PSCM) at the ILL is thanked for providing the microcalorimeter, the ellipsometer,

https://dx.doi.org/10.1021/acs.langmuir.0c01544
Langmuir 2020, 36, 10941−10951

and the quartz crystal microbalance. A.B., D.B., and C.M. acknowledge CSGI for the partial financial support.

REFERENCES

(1) Akbarzadeh, A.; Rezaei-sadabady, R.; Davaran, S.; Joo, S. W.; Zarghami, N.; Hanifehpour, Y.; Samiei, M.; Kouhi, M.; Nejati-Koshki, K. Liposome: classification, preparation, and applications. *Nanoscale Res. Lett.* **2013**, *8*, No. 102.
(2) Malam, Y.; Loizidou, M.; Seifalian, A. M. Liposomes and nanoparticles: nanosized vehicles for drug delivery in cancer. *Trends Pharmacol. Sci.* **2009**, *30*, 592−599.
(3) El Maghraby, G. M.; Barry, B. W.; Williams, A. C. Liposomes and skin: From drug delivery to model membranes. *Eur. J. Pharm. Sci.* **2008**, *34*, 203−222.
(4) Chan, Y.-H. M.; Boxer, S. G. Model membrane systems and their applications. *Curr. Opin. Chem. Biol.* **2007**, *11*, 581−587.
(5) Kang, M.; Tuteja, M.; Centrone, A.; Topgaard, D.; Leal, C. Nanostructured Lipid-Based Films for Substrate-Mediated Applications in Biotechnology. *Adv. Funct. Mater.* **2018**, *28*, No. 1704356.
(6) Kowal, J.; Wu, D.; Mikhalevich, V.; Palivan, C. G.; Meier, W. Hybrid Polymer − Lipid Films as Platforms for Directed Membrane Protein Insertion. *Langmuir* **2015**, *31*, 4868−4877.
(7) Richter, R. P.; Brisson, A. R. Following the Formation of Supported Lipid Bilayers on Mica: A Study Combining AFM, QCM-D, and Ellipsometry. *Biophys. J.* **2005**, *88*, 3422−3433.
(8) Montis, C.; Gerelli, Y.; Fragneto, G.; Nylander, T.; Baglioni, P.; Berti, D. Nucleolipid bilayers: A quartz crystal microbalance and neutron reflectometry study. *Colloids Surf., B* **2016**, *137*, 203−213.
(9) Discher, D. E.; Ahmed, F. Polymersomes. *Annu. Rev. Biomed. Eng.* **2006**, *8*, 323−341.
(10) Discher, B. M.; et al. "Polymersomes: Tough Vesicles Made from Diblock Copolymers,". *Science* **1999**, *284*, 1143−1146.
(11) Messager, L.; Gaitzsch, J.; Chierico, L.; Battaglia, G. "Novel aspects of encapsulation and delivery using polymersomes,". *Curr. Opin. Pharmacol.* **2014**, *18*, 104−111.
(12) Kim, Y.; et al. "Polymersome delivery of siRNA and antisense oligonucleotides,". *J. Controlled Release* **2009**, *134*, 132−140.
(13) Zhu, Y.; Yang, B.; Chen, S.; Du, J. "Polymer vesicles: Mechanism, preparation, application, and responsive behavior,". *Prog. Polym. Sci.* **2017**, *64*, 1−22.
(14) Chandrawati, R.; Caruso, F. "Biomimetic liposome- and polymersome-based multicompartmentalized assemblies,". *Langmuir* **2012**, *28*, 13798−13807.
(15) Rideau, E.; Dimova, R.; Schwille, P.; Wurm, F. R.; Landfester, K. "Liposomes and polymersomes: a comparative review towards cell mimicking,". *Chem. Soc. Rev.* **2018**, *47*, 8572−8610.
(16) Schulz, M.; Binder, W. H. "Mixed Hybrid Lipid/Polymer Vesicles as a Novel Membrane Platform,". *Macromol. Rapid Commun.* **2015**, *36*, 2031−2041.
(17) Dao, T. P. T.; et al. "Phase Separation and Nanodomain Formation in Hybrid Polymer/ Lipid Vesicles,". *ACS Macro Lett.* **2015**, *4*, 182−186.
(18) Shen, W.; Hu, J.; Hu, X. "Impact of amphiphilic triblock copolymers on stability and permeability of phospholipid/polymer hybrid vesicles,". *Chem. Phys. Lett.* **2014**, *600*, 56−61.
(19) Dao, T. P. T.; et al. "Modulation of phase separation at the micron scale and nanoscale in giant polymer/lipid hybrid unilamellar vesicles (GHUVs),". *Soft Matter* **2017**, *13*, 627−637.
(20) Schulz, M.; et al. "Hybrid lipid/polymer giant unilamellar vesicles: effects of incorporated biocompatible PIB − PEO block copolymers on vesicle properties,". *Soft Matter* **2011**, *7*, 8100−8110.
(21) Gettel, D. L.; et al. "Mixing, Diffusion, and Percolation in Binary Supported Membranes Containing Mixtures of Lipids and Amphiphilic Block Copolymers,". *J. Am. Chem. Soc* **2014**, *136*, 10186−10189.
(22) Mumtaz Virk, M.; Hofmann, B.; Reimhult, E. "Formation and Characteristics of Lipid-Blended Block Copolymer Bilayers on a Solid Support Investigated by Quartz Crystal Microbalance and Atomic Force Microscopy,". *Langmuir* **2019**, *35*, 739−749.
(23) Paxton, W. F.; McAninch, P. T.; Shin, S. H. R.; Brubach, M. T. "Adsorption and fusion of hybrid lipid/polymer vesicles onto 2D and 3D surfaces,". *Soft Matter* **2018**, *14*, 8112−8118.
(24) Khan, S.; Li, M.; Muench, S. P.; Jeuken, L. J. C.; Beales, P. A. "Durable proteo-hybrid vesicles for the extended functional lifetime of membrane proteins in bionanotechnology,". *Chem. Commun.* **2016**, *52*, 11020−11023.
(25) Beales, P. A.; Khan, S.; Muench, S. P.; Jeuken, L. J. C. "Durable vesicles for reconstitution of membrane proteins in biotechnology,". *Biochem. Soc. Trans.* **2017**, *45*, 15−26.
(26) Salvatore, A.; Montis, C.; Berti, D.; Baglioni, P. "Multifunctional Magnetoliposomes for Sequential Controlled Release,". *ACS Nano* **2016**, *10*, 7749−7760.
(27) Brinkhuis, R. P.; Rutjes, F. P. J. T.; van Hest, J. C. M. "Polymeric vesicles in biomedical applications,". *Polym. Chem.* **2011**, *2*, 1449−1462.
(28) Nagle, J. F.; Tristram-Nagle, S. "Structure of lipid bilayers,". *Biochim. Biophys. Acta, Rev. Biomembr.* **2000**, *1469*, 159−195.
(29) Magnani, C.; et al. "Hybrid vesicles from lipids and block copolymers: Phase behavior from the micro- to the nano-scale,". *Colloids Surf., B* **2018**, *168*, 18−28.
(30) Reeves, J. P.; Dowben, R. M. "Formation and Properties of Thin-walled Phospholipid Vesicles,". *J. Cell. Physiol.* **1969**, *73*, 49−60.
(31) Provencher, S. W. "Contin: a general purpose constrained regularization program for inverting noisy linear algebraic and integral equations,". *Comput. Phys. Commun.* **1982**, *27*, 229−242.
(32) Cisse, A.; Peters, J.; Lazzara, G.; Chiappisi, L. "PyDSC: a simple tool to treat differential scanning calorimetry data,". *J. Therm. Anal. Calorim.* **2020**, DOI: 10.1007/s10973-020-09775-9.
(33) Malakhov, D. V.; Khatwa, M. K. A. "Constructing a self-consistent integral baseline by using cubic splines,". *J. Therm. Anal. Calorim.* **2007**, *87*, 595−599.
(34) De Feijter, J. A.; Benjamins, J.; Veer, F. A. "Ellipsometry as a Tool to Study the Adsorption Behavior of Synthetic and Biopolymers at the Air- Water Interface,". *Biopolymers* **1978**, *17*, 1759−1772.
(35) Newville, M. et al.. *lmfit/lmfit-py 1.0.0*. Dec 2019.
(36) Byrnes, S. J. Multilayer optical calculations 2019, 1 20.
(37) Sauerbrey, G. "Verwendung von Schwingquarzen zur Wägung dünner Schichten und zur Mikrowägung,". *Zeitschrift für Phys.* **1959**, *155*, 206−222.
(38) Szoka, F.; Papahadjopoulos, D. "Comparative properties and methods of preparation of lipid vesicles (liposomes),". *Annu. Rev. Biophys. Bioeng.* **1980**, *9*, 467−508.
(39) Bartenstein, J. E.; Robertson, J.; Battaglia, G.; Briscoe, W. H. "Stability of polymersomes prepared by size exclusion chromatography and extrusion,". *Colloids Surf., A* **2016**, *506*, 739−746.
(40) Lewis, R. N.; Pohle, W.; Mcelhaney, R. N. "The Interfacial Structure of Phospholipid Bilayers: Differential Scanning Calorimetry and Fourier Transform Infrared Spectroscopic Studies of 1, 2-Dipalmitoyl-sn-Glycero-3-Phosphorylcholine and Its Dialkyl and Acyl-Alkyl Analogs,". *Biophys. J.* **1996**, *70*, 2736−2746.
(41) Riske, K. A.; Barroso, R. P.; Vequi-Suplicy, C. C.; Germano, R.; Henriques, V. B.; Lamy, M. T. "Lipid bilayer pre-transition as the beginning of the melting process,". *Biochim. Biophys. Acta, Biomembr.* **2009**, *1788*, 954−963.
(42) Mabrey, S.; Sturtevant, J. M. "Investigation of phase transitions of lipids and lipid mixtures by high sensitivity differential scanning calorimetry,". *Proc. Natl. Acad. Sci. U.S.A.* **1976**, *73*, 3862−3866.
(43) MacDonald, R. C.; Simon, S. A. "Lipid monolayer states and their relationships to bilayers,". *Proc. Natl. Acad. Sci. U.S.A.* **1987**, *84*, 4089−4093.
(44) Feng, S.-s. "Interpretation of Mechanochemical Properties of Lipid Bilayer Vesicles from the Equation of State or Pressure - Area Measurement of the Monolayer at the Air - Water or Oil - Water Interface,". *Langmuir* **1999**, *15*, 998−1010.
(45) Iyer, J.; Hammond, P. T. "Langmuir Behavior and Ultrathin Films of New Linear-Dendritic Diblock Copolymers,". *Langmuir* **1999**, *15*, 1299−1306.

https://dx.doi.org/10.1021/acs.langmuir.0c01544
Langmuir 2020, 36, 10941−10951

(46) Rodríguez-García, R.; Mell, M.; López-Montero, I.; Netzel, J.; Hellweg, T.; Monroy, F. "Polymersomes: smart vesicles of tunable rigidity and permeability,". *Soft Matter* **2011**, *7*, 1532−1542.
(47) Matmour, R.; Francis, R.; Duran, R. S.; Gnanou, Y. "Interfacial Behavior of Anionically Synthesized Amphiphilic Star Block Copolymers Based on Polybutadiene and Poly (ethylene oxide) at the Air / Water Interface,". *Macromolecules* **2005**, *38*, 7754−7767.
(48) Ahmed, F.; Hategan, A.; Discher, D. E.; Discher, B. M. "Block Copolymer Assemblies with Cross-Link Stabilization: From Single-Component Monolayers to Bilayer Blends with PEO-PLA,". *Langmuir* **2003**, *19*, 6505−6511.
(49) Vollhardt, D.; Fainerman, V. B. "Progress in characterization of Langmuir monolayers by consideration of compressibility,". *Adv. Colloid Interface Sci.* **2006**, *127*, 83−97.
(50) Abraham, T.; Schooling, S. R.; Beveridge, T. J.; Katsaras, J. "Monolayer Film Behavior of Lipopolysaccharide from Pseudomonas aeruginosa at the Air-Water Interface,". *Biomacromolecules* **2008**, *9*, 2799−2804.
(51) Ali, S.; Smaby, J. M.; Momsen, M. M.; Brockman, H. L.; Brown, R. E. "Acyl Chain-Length Asymmetry Alters the Interfacial Elastic Interactions of Phosphatidylcholines,". *Biophys. J.* **1998**, *74*, 338−348.
(52) Richter, R. P.; Bérat, R.; Brisson, A. R. "Formation of Solid-Supported Lipid Bilayers: An Integrated View,". *Langmuir* **2006**, *22*, 3497−3505.
(53) Willes, K. L.; Genchev, J. R.; Paxton, W. F. "Hybrid lipid-polymer bilayers: pH-mediated interactions between hybrid vesicles and glass,". *Polymers* **2020**, *12*, No. 745.
(54) Montis, C.; et al. "Biogenic Supported Lipid Bilayers from Nanosized Extracellular Vesicles,". *Adv. Biosyst.* **2018**, *2*, No. 1700200.
(55) Reviakine, I.; Johannsmann, D.; Richter, R. P. "Hearing what you cannot see and visualizing what you hear: Interpreting quartz crystal microbalance data from solvated interfaces,". *Anal. Chem.* **2011**, *83*, 8838−8848.

https://dx.doi.org/10.1021/acs.langmuir.0c01544
Langmuir 2020, 36, 10941−10951